SOFT ROBOTICS
Volume 00, Number 00, 2023

DOI: 10.1089/soro.2022.0134

SoRo
Soft Robotics

Open camera or QR reader and scan code to access this article and other resources online.

JamTac: A Tactile Jamming Gripper for Searching and Grasping in Low-Visibility Environments

Shoujie Li,[1,†] Linqi Ye,[2,†] Haixin Yu,[1] Xianghui Yin,[1] Chongkun Xia,[1] Wenbo Ding,[1] Xueqian Wang,[1] and Bin Liang[3]

Abstract

Humans can feel and grasp efficiently in the dark through tactile feedback, whereas it is still a challenging task for robots. In this research, we create a novel soft gripper named JamTac, which has high-resolution tactile perception, a large detection surface, and integrated sensing-grasping capability that can search and grasp in low-visibility environments. The gripper combines granular jamming and visuotactile perception technologies. Using the principle of refractive index matching, a refraction-free liquid-particle rationing scheme is developed, which makes the gripper itself to be an excellent tactile sensor without breaking its original grasping capability. We simultaneously acquire color and depth information inside the gripper, making it possible to sense the shape, texture, hardness, and contact force with high resolution. Experimental results demonstrate that JamTac can be a promising tool to search and grasp in situations when vision is not available.

Keywords: soft robotics, jamming gripper, tactile sensing, universal grasping

Introduction

Grasping is one of the most important ways for people and robots to interact with the world. Humans make extensive use of multisensory feedback during grasping, including visual and tactile sensing.[1] Although vision is the most important source of information, it is not so reliable and becomes inefficient in low-visibility environments. On the contrary, tactile sensing, just like proprioceptive sense,[2] is more robust and reliable compared to vision. Tactile perception can provide accurate contact information such as texture and force, which improves the grasping performance.[3] More importantly, tactile sensing plays a crucial role in the grasping behavior when vision is lacked, such as in dark night, turbid water, and dense smoke. In practice, there is a vast demand for operations in low-visibility conditions, for example, object salvage in muddy water, target searching in fire disasters, valve manipulation in toxic gas leakage, and so on. Working in those environments is typically hard and dangerous. Therefore, it is of great significance to develop robotic grippers that are capable of searching and grasping in low-visibility environments.

[1]Center of Intelligent Control and Telescience, Tsinghua Shenzhen International Graduate School, Tsinghua University, Shenzhen, China.
[2]Institute of Artificial Intelligence, Collaborative Innovation Center for the Marine Artificial Intelligence, Shanghai University, Shanghai, China.
[3]Navigation and Control Research Center, Department of Automation, Tsinghua University, Beijing, China.
[†]These authors contributed equally to this work.

In the field of robotic grasping, while many research focus on the use of computer vision to achieve object grasping,[4–7] tactile sensors[8–10] also have attracted enormous interest. Tactile sensors can be divided into piezoresistive,[11] capacitive,[12] inductive,[13] etc. Although they have high accuracy for force detection, the resolution for texture detection is usually low. To improve the resolution, optical tactile sensors, including soft marker-based optical tactile sensors and soft reflection-based optical tactile sensors,[14] have been proposed, which use a built-in camera to obtain the deformation information of the contact surface. This method has high resolution, as well as low cost, making it suitable for large-scale applications. Various optical tactile sensors have emerged, such as GelForce,[15] Digit,[16] Gelsight,[17] Omnitact,[18] TacTip,[19] and Insight.[20] However, the detection area of those sensors is small and the ductility of the surface silicone film is poor, making it difficult to obtain the 3D contour information for irregular objects.

Currently, tactile sensors have been applied to various grippers, with most of them being rigid grippers.[21–25] At present, rigid grippers[26–30] are widely used in the industrial field due to their superior load capacity, high accuracy, and durability. However, they have poor flexibility and might cause harm to the object. On the contrary, soft grippers[31–35] are highly flexible and allow safe interaction between robots and the environments. But the integration of tactile sensors with soft grippers is still a challenging task.[36–39] There are various types of soft grippers such as pneumatic elastomeric grippers,[40] electrostatic actuated grippers,[41] shape memory polymer driven grippers,[42] and jamming grippers.[43–46] Among them, the jamming gripper consists of a soft package filled with particles and uses the jamming effect to change the stiffness of the gripper to achieve gripping. Unlike the finger-shaped gripper, jamming grippers have a relatively large contact surface that can easily wrap the object, which greatly reduces the planning work during grasping. Jamming grippers have a broad application prospect from industrial applications[47] to deep sea sampling.[48]

Integrating tactile sensing into jamming grippers is an interesting research direction, where Ref.[49] is the first to introduce an optical tactile version of a particle jamming gripper. However, for jamming grippers, the surface material should be thin and flexible, making it extremely difficult to add a suitable tactile sensor without affecting the grasping performance. There are two possible ways to achieve this. The first is to add a highly flexible electronic skin on its surface, such as the conductive thermoplastic elastomer.[50] In this way although the gripper can have tactile perception, the added electronic components will greatly degrade its gripping performance and the complex wirings will also affect the durability of the gripper.

The second is to add a camera inside the gripper to observe the deformation of the membrane to obtain tactile

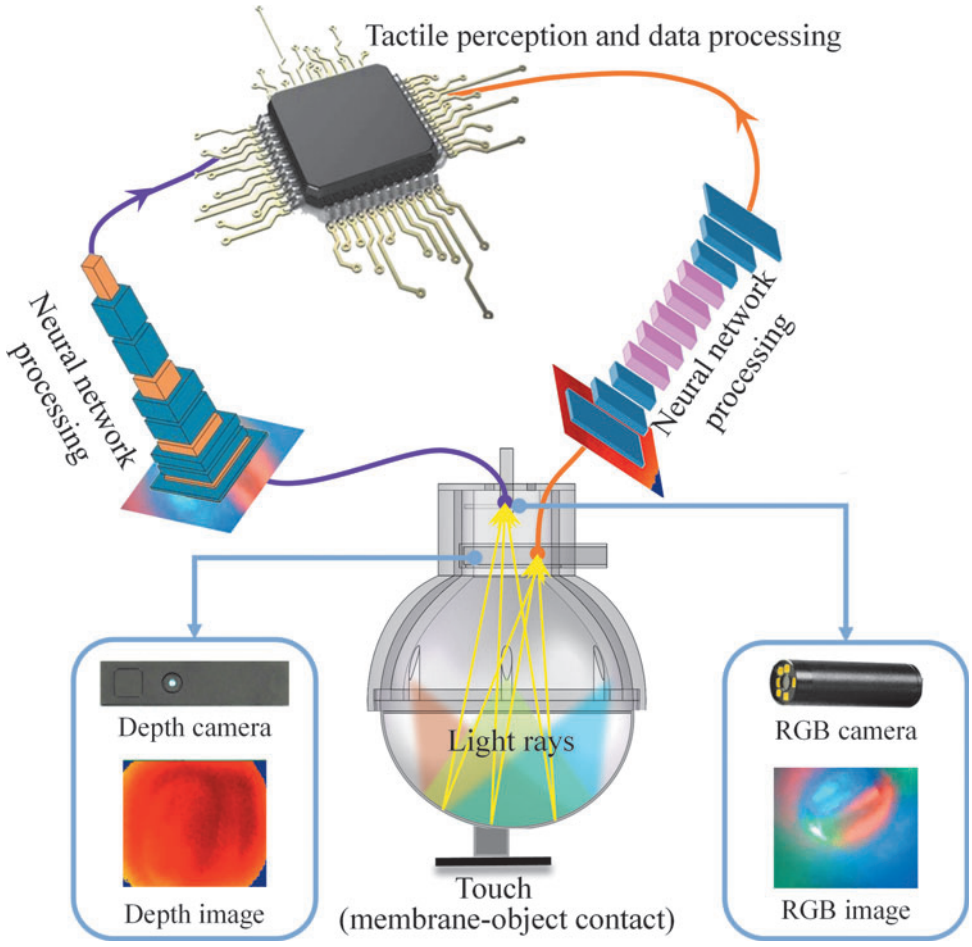

FIG. 1. Basic principle of JamTac. Color and depth images are obtained simultaneously inside the gripper to output tactile sensing information.

information, which does not affect the gripping performance. However, in this way the internal particles will obstruct the view of the camera, making the resolution extremely low. Although a method has been proposed to make the interior transparent using acrylic and mixed paraffin-silicone oil as the filling material,[51] the resolution is still far from satisfactory. Besides, the selected mixture has poor fluidity and contains impurities. Therefore, it still requires large improvement to achieve high-resolution tactile perception for jamming grippers.

In this work, we leverage the visuotactile technology to promote the tactile sensing capability of the jamming gripper to a new level. We apply both RGB (red, green and blue) color camera and depth camera inside the gripper, resulting in the gripper JamTac as shown in Figure 1. JamTac differs from other grippers/sensors in three main aspects. First, the gripper has high-resolution tactile sensing capability compared to other jamming grippers. This is achieved by adopting a novel mixture of liquid and particles with matched refractive index as the internal filler, which is highly transparent, fluidity-well, nontoxic, and noncorrosive. Second, the gripper has integrated sensing and grasping capability. It can feel and then grasp irregularly shaped objects easily by pumping the liquid (Supplementary Movie S1). Third, the gripper can obtain the 3D contour information of the object through a single contact due to its wide and largely-

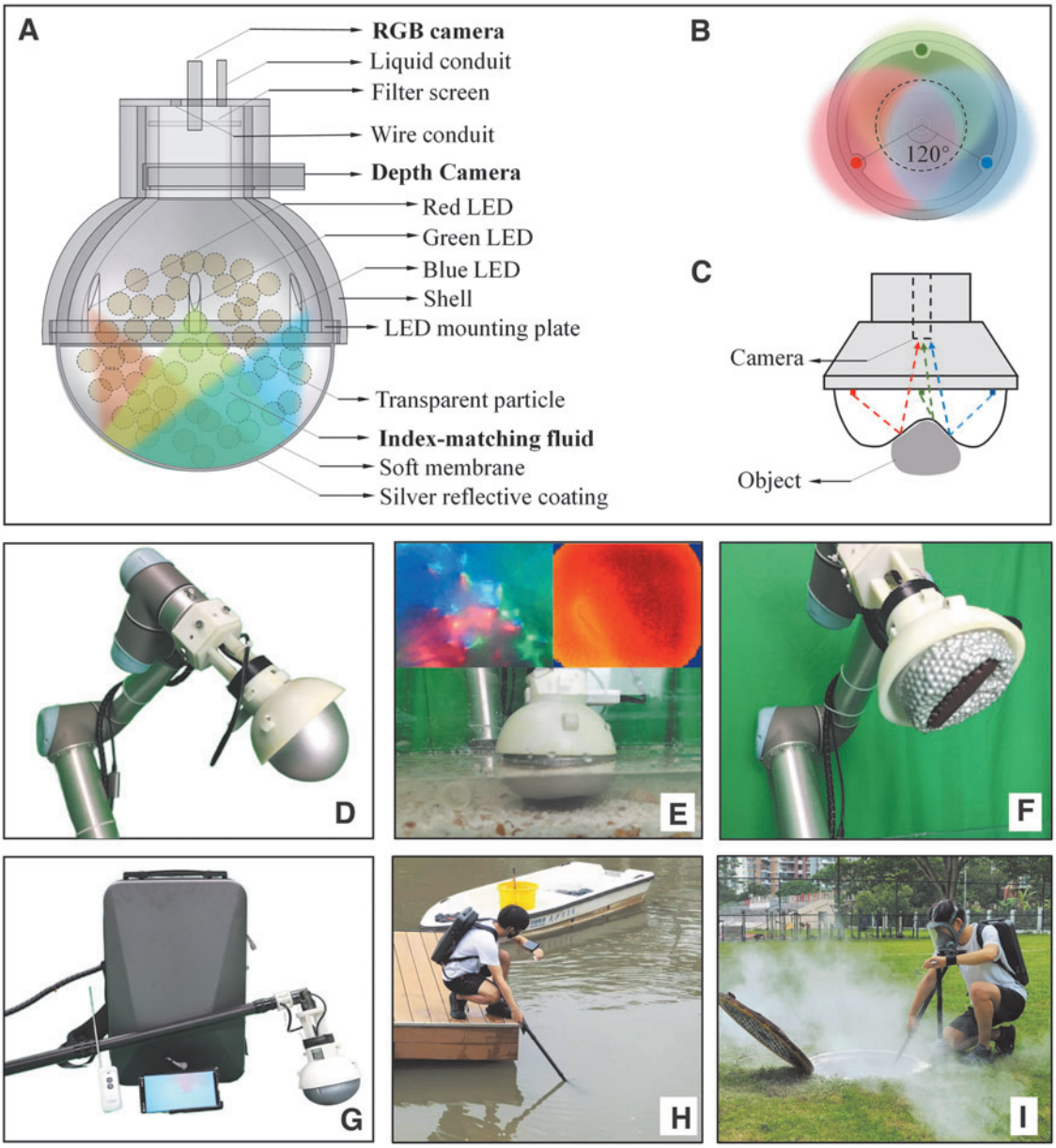

FIG. 2. The proposed gripper JamTac. **(A)** The structure of JamTac. **(B)** The layout of the LED plane. **(C)** The light path inside the gripper. **(D)** The gripper attached to a UR5 robotic arm. **(E)** The gripper in sensing mode and the images from cameras inside the gripper. **(F)** The gripper in grasping mode. **(G)** The underwater salvage equipment. **(H)** Using the equipment to salvage in a river. **(I)** Using the equipment to operate in a sewer well with smoke.

deformable membrane surface (Supplementary Movie S1), which can be hardly achieved by other tactile sensors as far as we know. All of the above features make JamTac an excellent tool to facilitate searching and grasping tasks in low-visibility environments.

Gripper Design

The fabrication process of JamTac can be found in Supplementary Figure S1. Traditional jamming grippers are composed of three main components, which are particles, elastic film, and shell. To achieve high-quality tactile perception, we make several delicate modifications. As shown in Figure 2A, LEDs and cameras are added, and the internal filler is replaced by a mixture of liquid and particles, which looks highly transparent from the camera, and the inner side of the elastic film is covered with silver reflective coatings.

Our goal is to design a jamming gripper with the sense of shape, texture, hardness, and force. To achieve this, we have been motivated from Gelsight,[17] which is a soft reflection-based optical tactile sensor with a high spatial resolution up to 1 micron. Gelsight uses an RGB camera, but it is highly sensitive to depth by taking advantage of the photometric stereo technique. However, unlike Gelsight, a jamming gripper has highly flexible curved surface filled with particles inside, preventing it from applying photometric stereo. Therefore, we apply both RGB and depth cameras inside the gripper. RGB camera has high resolution and fineness, which is sensitive to information such as texture and shape of the contact surface. While depth camera has low resolution, it can reconstruct the 3D morphology of the gripper surface (Supplementary Movie S2) and obtain information such as 3D contour, hardness, and force. Therefore, the combination of depth camera and RGB camera can simultaneously achieve shape/texture detection, hardness perception, and force perception.

Our main concerns for the selection of the RGB camera are waterproof performance, volume, and field of view. To better detect the deformation of the gripper surface, the camera needs to be immersed in the liquid, which puts severe

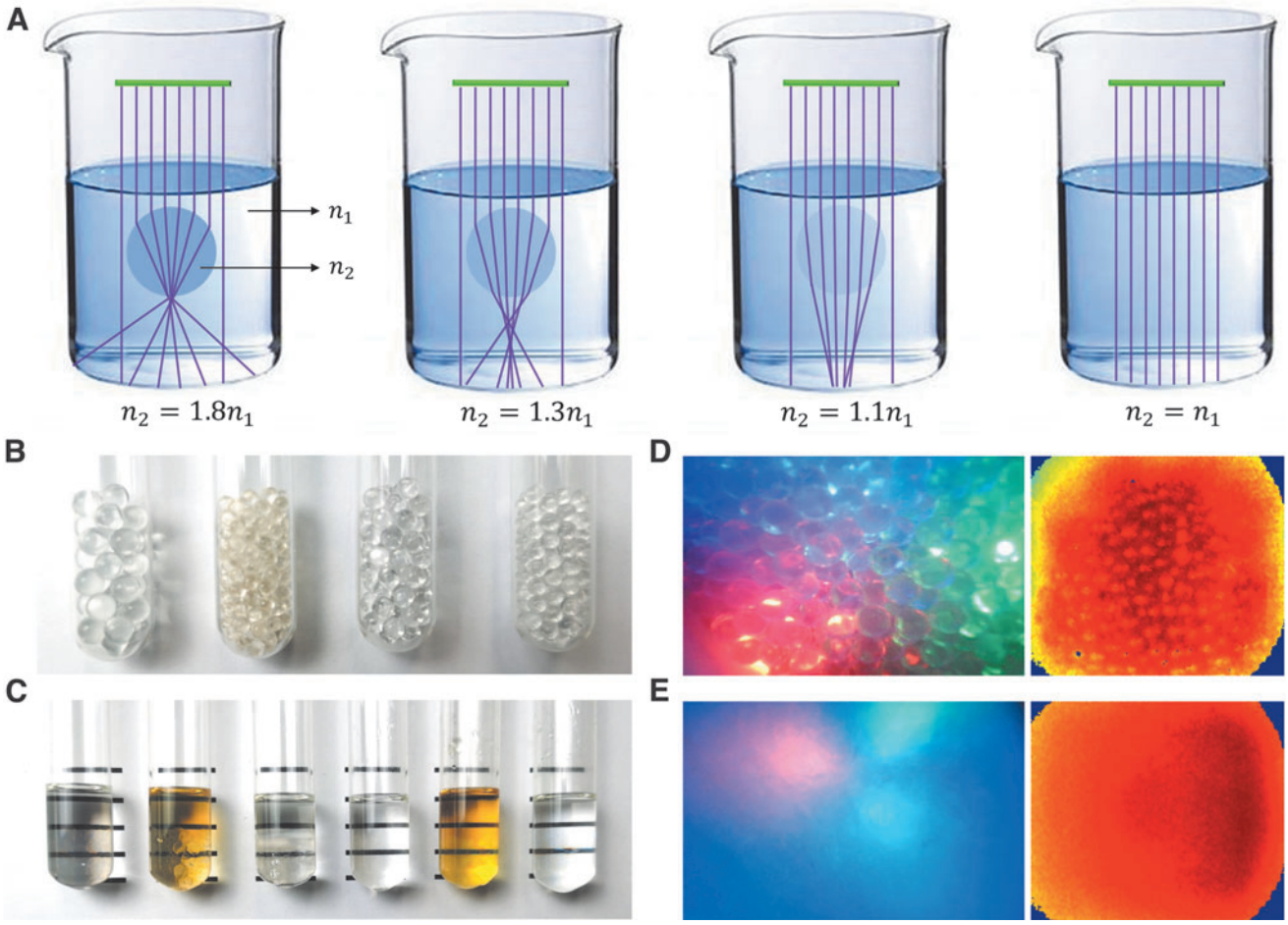

FIG. 3. Particles, solutions, and camera views. **(A)** Light rays pass through liquid with solid beads. As the refractive index of the bead gets closer to that of the liquid, the light is less deflected and the bead becomes less visible. Particularly, when $n_2 = n_1$, the bead becomes invisible. **(B)** The particles alone. *Left to right*: H-K9 glass, organic glass, high borosilicate glass, super absorbent resin. **(C)** The mixture of particles and liquid. *Left to right*: 87.25% tetralin-ethanol solution and H-K9 glass, 12.4% engine oil-benzene solution and organic glass, p-cymene and organic glass, water and super absorbent resin, 59% NaI solution and high borosilicate glass, 59% NaI solution and high borosilicate glass with $Na_2S_2O_3$ as a decolorizer. **(D)** The RGB and depth images captured from inside the gripper when there is no liquid. **(E)** The RGB and depth images from inside the gripper are clean when there is index-matching liquid.

requirements on the waterproof performance of the camera. In addition, the space in the gripper is very limited, and thus, how to install both depth camera and color camera in it is an important issue. Eventually, the RGB camera selected is a 120° wide-angle endoscopic camera with a resolution of 1920×1080, a frame rate of 30 fps. The diameter of this camera is only 8.5 mm. It also has a good waterproof property and can work in underwater high-pressure environments. The depth camera selected is CamBoardpicoflexx with a size of $68 \times 17 \times 7.25$ mm, which can be easily integrated into the gripper. The highest frame rate of the depth camera can reach 45 fps, and the minimum detection range is 100 mm (the distance between the depth camera and the bottom of the balloon is 120 mm).

In addition to the cameras, the design of the elastic film of the gripper is also one of the critical aspects that affect the tactile sensing performance. Currently, most of the optical tactile sensors use transparent glass with a layer of silicone, which is easy to fabricate, but is less flexible and can hardly adapt to objects with irregular shapes. Here an elastic latex film with a silver reflective coating is adopted, which has better reflectivity and results in more uniform internal lighting and a clearer view of the textures. The film is very flexible with a thickness of merely 0.25 mm, which enables it to sense tiny texture information on the surface of the grasped object. Furthermore, to improve the brightness and visual effect inside the gripper, RGB LEDs of flat head and fog light are adopted. The three LEDs are evenly spaced along a circle, and the brightness of the light emitted by this type of LED is more uniform, which can avoid the impact of traditional LED spotlighting.

Internal Filler Design

To allow the camera to observe the membrane deformation clearly, we need to keep the internal filler of the gripper transparent. While it is difficult for solid particles to be unseen in the air, making them ''disappear'' in liquid is possible. The key lies in the refractive index. If the refractive indexes of the particles and the liquid are the same, then the particles will be invisible.[52]

The refractive index is an inherent property of the material, which is defined as the ratio of the propagation speed of light in a vacuum to the propagation speed of light in the material medium. The higher the refractive index of the material, the greater the refraction of the transmitted light through the material. Usually, the refractive index order is ''solids > liquids > gases.''

Figure 3A shows light rays passing through liquid with particle (both are transparent and have the same color), where n_1 represents the refractive index of the liquid and n_2 denotes the refractive index of the particle. When light is transmitted from the liquid into the particle, refraction and reflection happen at the particle's surface because there is a difference in refractive index. Therefore, we can notice that there is a particle because its edge is highlighted (due to reflection) and the background behind the particle is distorted (due to refraction). As the refractive index of the particle gets closer to that of the liquid, the light is less deflected and the particle becomes less visible. When the liquid and the particle have the same refractive index, then no refraction or reflection occurs at the interface, thus the particle appears to disappear. This phenomenon is demonstrated in Supplementary Movie S3.

Particularly, if the liquid is a compound, then its refractive index can be calculated using the Lorentz-Lorenz formula[53]:

$$\frac{n^2-1}{n^2+2} = \sum_{i=1}^{N} \varphi_i \frac{n_i^2-1}{n_i^2+2} \tag{1}$$

where n is the refractive index of the mixture, n_i is the refractive index of the *i-th* component, and φ_i is the volume fraction. Using this formula, we can find a series of liquid-particle pairs that have an equal refractive index (also called refractive index matching) as shown in Table 1. They can serve as candidates for the internal filler, and the defects are also listed in the table.

To obtain an internal filler that is stable, nontoxic, transparent, and has good flow ability, we tested six of the refractive index matching mixtures with the results shown in Figure 3C. It can be observed that the mixtures are transparent. However, as listed in Table 1, most of them have problems such as dissolution, volatilization, discoloration, and poor flow ability. For example, tetralin can dissolve organic materials such as elastic film, hoses, and pumps, thus causing leakage; p-toluene and benzene can make the elastic film swell, thus breaking the elasticity of the film; engine oil-benzene solution has poor liquidity and is difficult to be extracted quickly through the pump; water and super absorbent resin have no such problem, but the resin will become soft

Table 1. Liquid-Particle Pairs with Refractive Index Matching

Liquid material	*Particle material*	*Refractive index*	*Defect*
Water	Super absorbent resin	1.333	Particle is too soft
59% NaI solution	High borosilicate glass	1.473	Oxidized to brown
59.37% tetrachloromethane-tetrahydrofuran solution	Fluorine crown glass (CDGM mark: FK-95 [http://www.cdgmgd.com/])	1.438	Generate virulent phosgene
77.26% trichloromethane-tetrahydrofuran solution			
30.2% gasoline-benzene solution	Barium fluoride	1.474	Dissolve rubber film
12.4% engine oil-benzene solution	Organic glass	1.49	
p-cymene	Organic glass		
43.99% tetralin-ethanol solution	Fluorine crown glass (CDGM mark: H-FK95N)	1.438	Dissolve most organics
54.46% tetralin-ethanol solution	Fluorine crown glass (CDGM mark: H-FK71)	1.457	
76.64% tetralin-ethanol solution	Fluorine crown glass (CDGM mark: H-FK61)	1.497	
78% tetralin-ethanol solution	Fluorine crown glass (CDGM mark: H-K1)	1.499	
87.25% tetralin-ethanol solution	Fluorine crown glass (CDGM mark: H-K9)	1.517	

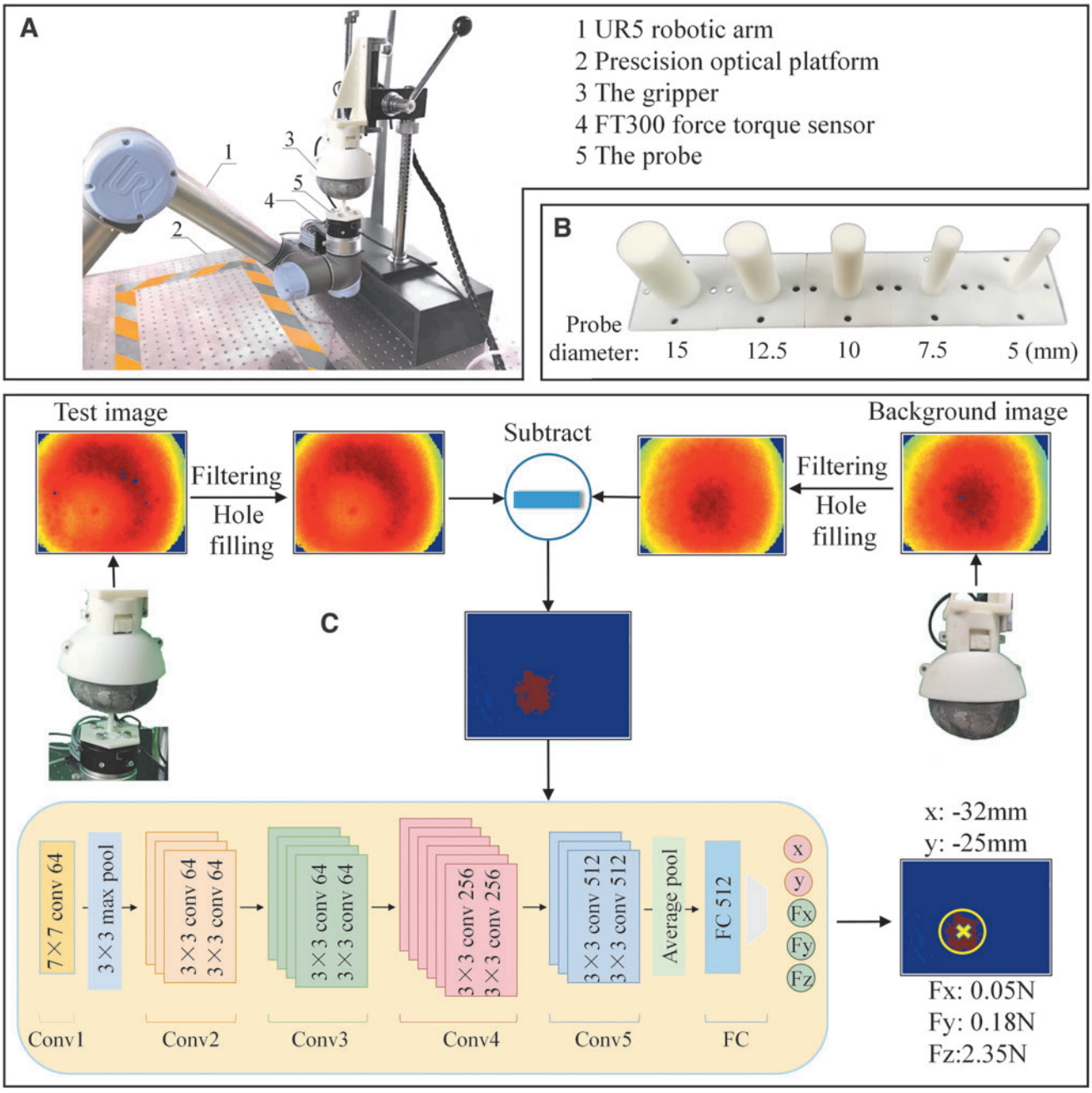

FIG. 4. Force sensing platform and method. **(A)** The autonomous force sensing platform. **(B)** Probes used for test with different diameters. **(C)** Depth image processing workflow.

after absorbing water, which will make the gripper lose the ability to grasp. After comprehensive consideration, we finally chose the combination of 59% NaI solution and high borosilicate glass as the filling materials.

The properties of NaI are similar to NaCl, but I^- has stronger reducibility, which is very easy to react with air and produce I_2. The process is as follows: $4NaI + O_2 + 2H_2O \rightarrow 4\,NaOH + 2\,I_2$. The generated I_2 can make the solution yellow and affect the transparency. To solve this problem, we add $Na_2S_2O_3$ which has stronger reducibility to the solution to prevent the solution from oxidation. The underlying mechanism can be shown as $2Na_2S_2O_3 + I_2 \rightarrow Na_2S_4O_6 + 2\,NaI$.

Because the solution in the gripper is not in contact with the outside air, we found adding 0.5% of $Na_2S_2O_3$ can maintain the solution in a colorless and transparent state for a long time without changing the refractive index much. Therefore, the final internal filler is a solution of 59% NaI mixed with 0.5% $Na_2S_2O_3$ and high borosilicate glass beads.

With this internal filler, Figure 3E shows the pictures from inside the gripper obtained by the RGB and depth cameras. As a comparison, we also show the pictures when there is no liquid (Fig. 3D). It can be seen that the camera view becomes clear and the particles are hidden when the particles are immersed in the liquid, which verifies the feasibility of the internal filler design.

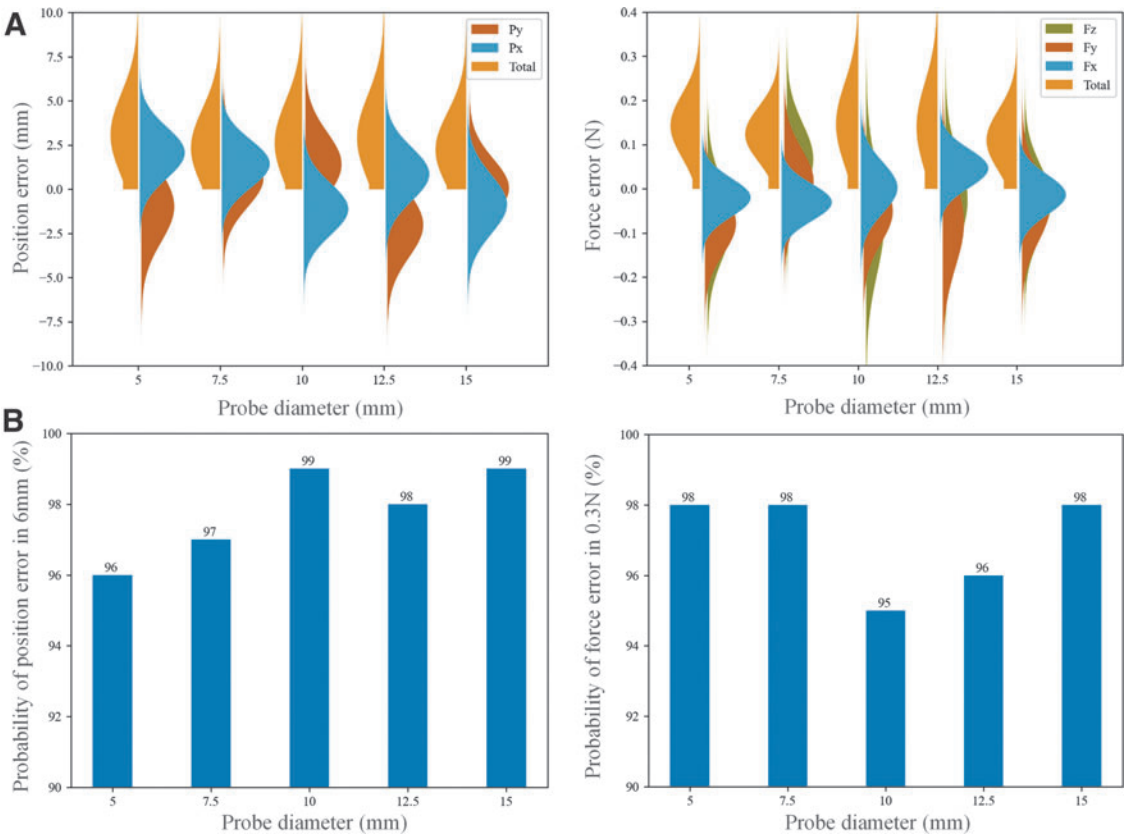

FIG. 5. Force sensing performance. **(A)** The position and force error distribution grouped by probe diameter. **(B)** The probability of position and force error (total) in a small region grouped by probe diameter.

Force Sensing Performance

Force sensing is an important aspect of tactile perception. For soft grippers, it is usually hard to mount traditional force sensors due to their flexible structure. However, a soft gripper itself can act as a force-sensing component by measuring the deformation during contact. For JamTac, which is composed of liquid, particles, and elastic film, it is very difficult to build an accurate force sensing model from First Principles. Therefore, a neural network-based force sensing method is proposed for JamTac. Since the contact status of the gripper is well described by the depth image, it can be used as input to train a force-sensing model.

The objects in real life usually have various shapes, and the contact status with the gripper can be very complicated. To simplify the problem, five cylindrical probes with different diameters are adopted as the testing objects (Fig. 4B). Neural network models are trained for each probe, which takes the depth image as input and outputs the 3D contact force information, as well as the contact position. The raw images for the experiments are given in Supplementary Data, and the neural network training details for each task can be found in Supplementary Table S1. We then test the trained model and apply Gaussian fitting to the sensing error distribution (The experimental process is shown in Supplementary Movie S4). The position and force error distribution are given in Figure 5A. It can be observed that the position error keeps within 10 mm, and the force error maintains below 0.4 N. Moreover, as the probe diameter increases from 5 to 15 mm (the gripper membrane has a diameter of about 90 mm), the force sensing performance is almost the same. As shown in Figure 5B, the probabilities of position error in 6 mm and the force error in 0.3 N are all above 95%. Moreover, the root mean square errors (RMSEs) for the position and force sensing are shown in Table 2.

Shape and Texture Recognition Performance

Compared to traditional jamming grippers, the main advantage of JamTac is its high-resolution shape/texture sensing capability. To test the performance, six objects with different shapes and textures are used as shown in Figure 6A. The corresponding RGB images obtained from inside the gripper are shown in Figure 6B. It can be seen that the RGB images show ultrahigh fidelity to the original objects. The noises

Table 2. Root Mean Square Errors for the Position and Force Sensing

Probe diameter (mm)	*Position error RMSE (mm)*	*Force error RMSE (N)*
5	3.363	0.160
7.5	2.638	0.138
10	2.949	0.174
12.5	3.227	0.172
15	2.500	0.130
Average	2.935	0.155

RMSE, root mean square error.

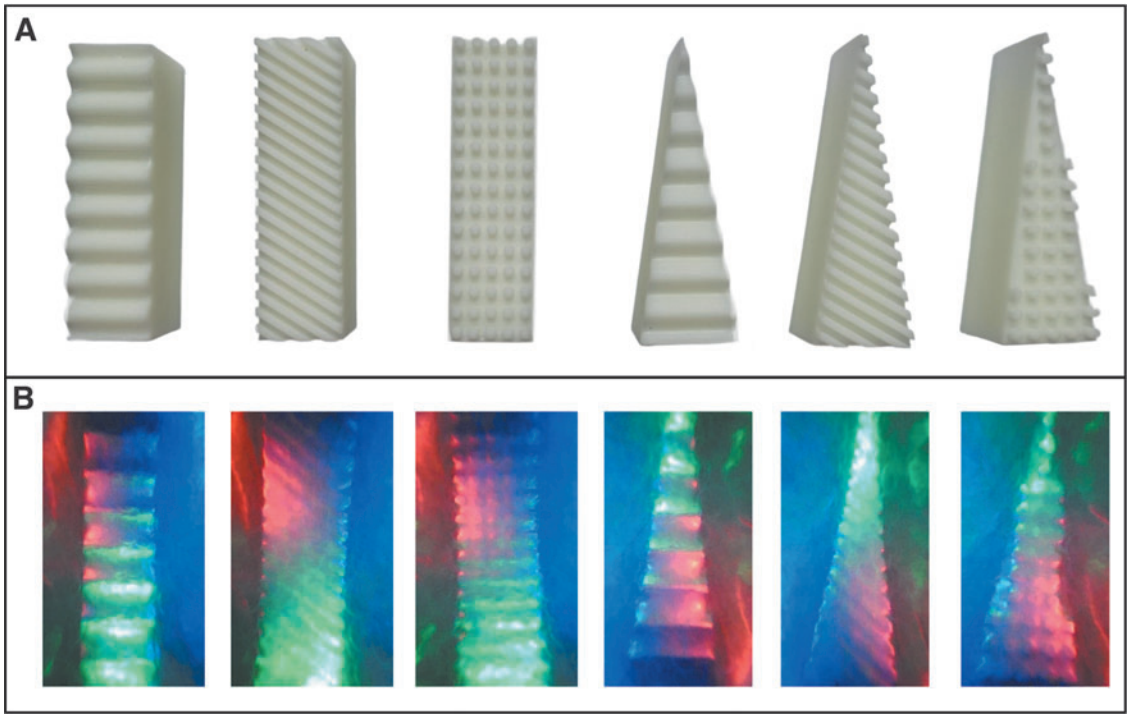

FIG. 6. Shape and texture recognition task. **(A)** Objects used for testing. *Left to right*: cuboid prism with wavy texture, cuboid prism with diagonal protrusions, cuboid prism with granular protrusions, triangular prism with wavy texture, triangular prism with diagonal protrusions, triangular prism with granular protrusions. **(B)** RGB images from inside the gripper when in contact with each object.

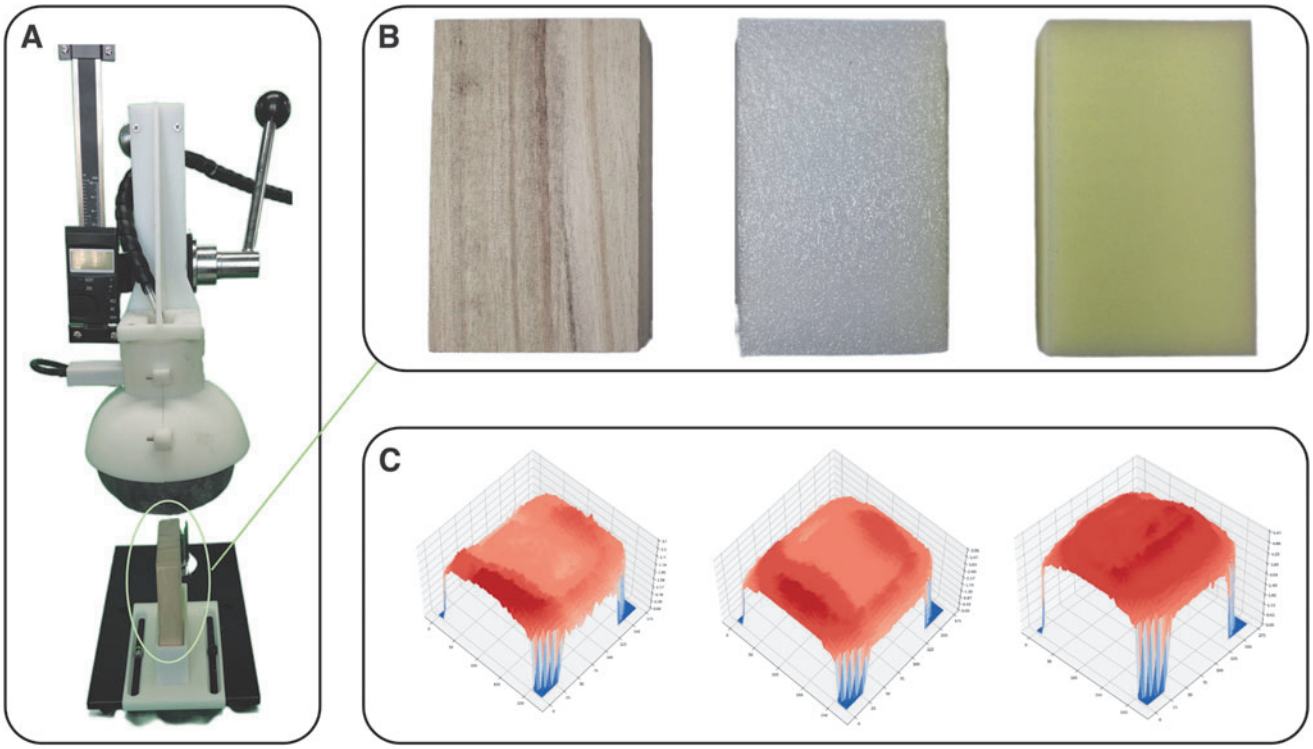

FIG. 7. Hardness identification task. **(A)** Experimental platform. **(B)** Hardness test material. *Left to right*: wood, foam, sponge. **(C)** Depth images from the gripper in contact with objects of different hardness. *Left to right*: wood, foam, and sponge.

in the RGB images maintain at a low level, and we can easily recognize the shape and texture from the image. It demonstrates JamTac's superior shape/texture sensing capability.

Furthermore, we also performed a classification task. The GoogleNet classification network was used. The input of the network is the RGB image from the gripper camera, and the output is the type of the grasped object. Two hundred images were collected for each object, resulting in 1200 images in total, where 240 of them were used as the test set. After 40 rounds of training, the shape/texture recognition accuracy achieved 98.8%, which validates the feasibility of the gripper for shape and texture recognition.

Hardness Identification Performance

Hardness detection can help robots to evaluate the property of the object and grasp the object more accurately. One promising application field of hardness detection is nondestructive fruit firmness evaluation.[54] The hardness of an object can be estimated through the deformation produced when the gripper contacts the object. Since the softer the object, the easier it is to deform, a softer object will bend more in the process of continuous downward pressure, which can be detected by the depth camera. Using this phenomenon, an experiment is designed to classify objects according to their hardness.

The tested objects are three cuboid substances made of wood, foam, and sponge, respectively, as shown in Figure 7B. The obtained depth images are given in Figure 7C. Since the deformation of the three objects is different, the depth images exhibit obvious differences. Similar to the previous experiment, the classification of objects is achieved using GoogleNet. In this experiment, 48 pictures were collected for each object, resulting in a total of 144 pictures, 36 of which were used as the test set. As a result, the success rate of recognition reached 100%.

Autonomous Searching and Grasping Test

One main advantage of the proposed gripper compared to the grippers using external vision is its effectiveness in low-

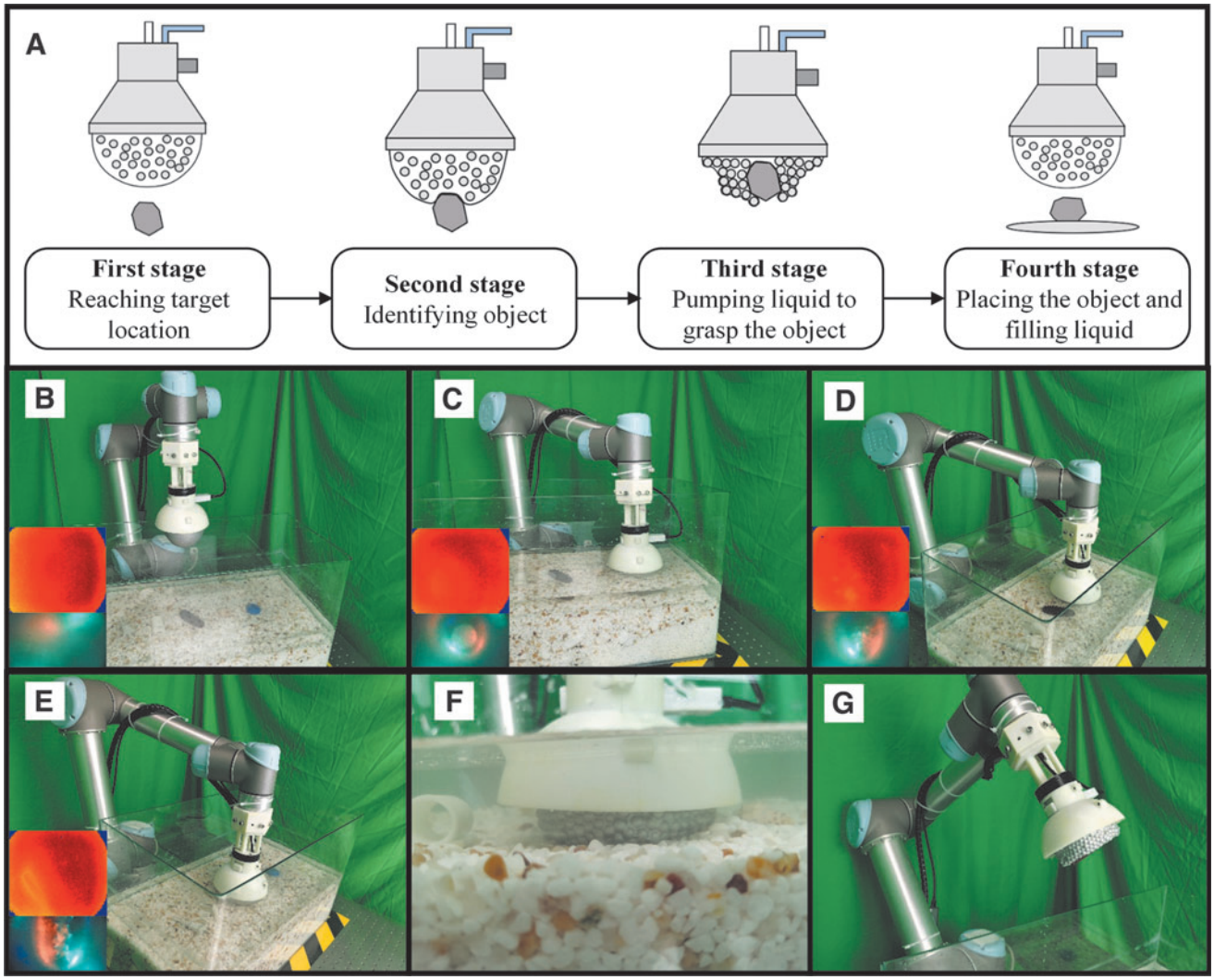

FIG. 8. The experimental process of the autonomous searching and grasping task. **(A)** The operation process. **(B)** The gripper in the initial position. **(C)** The gripper touches and recognizes the object, which is not the target object. **(D)** The gripper leaves the object and goes to the next detect position. **(E)** The gripper detects the target object. **(F)** The gripper pumps out liquid and grasps the object. **(G)** The gripper places the object in a specified location.

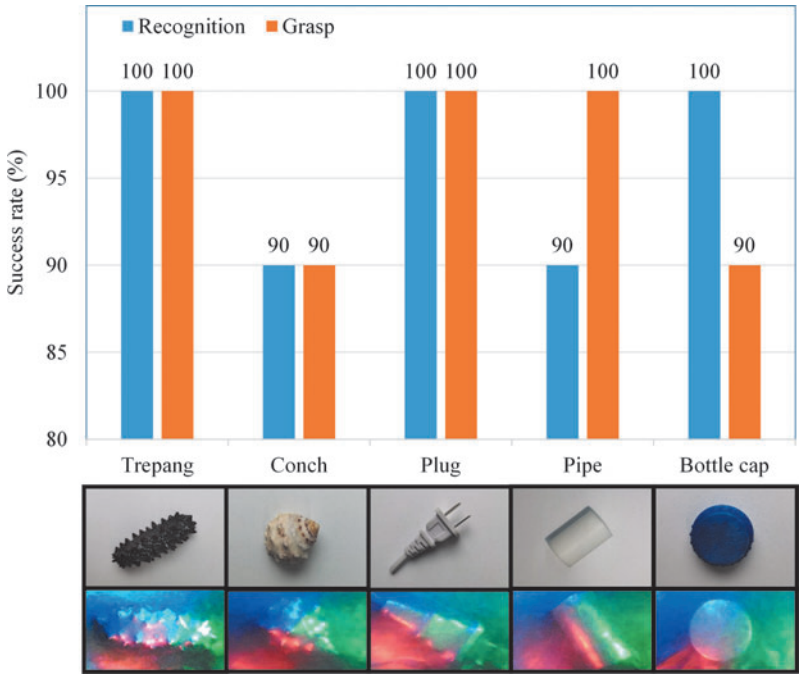

FIG. 9. The success rate of recognition and grasping.

visibility environments, just like people can search and grasp in the dark using their hands. To check the blind grasping performance of JamTac, an autonomous searching and grasping experiment is performed.

Five objects are selected in the experiment, including a trepang model (soft model), a conch (specimen), a plug, a pipe, and a bottle cap. Before the experiment, a classification network was built based on GoogleNet. Two hundred images were collected for each object, resulting in a total of 1000 images, where 200 of them were used as the test set. After training, the classification accuracy achieved 99%. Then the autonomous searching and grasping experiment was performed based on the trained classification network.

The operation process of the gripper in this experiment is shown in Supplementary Movie S5 and Figure 8. The process is divided into four stages. In the first stage, the gripper is in the initial position and slowly descends, using the classification algorithm to check whether it touches the target object during the descent. If the gripper detects no object, it moves to the next position and continues searching until it detects an object. In the second stage, the detected object will be classified. If it is the target object, it will be grasped. In the third stage, the liquid in the gripper is pumped out so that the gripper can hold the object firmly due to the jamming effect. In the fourth stage, the grasped object will be transferred to a specified location, and the liquid will be injected into the gripper to recover it to the sensing mode.

The experimental results are given in Figure 9. Ten tests are taken for each object. Among the total 50 experiments, 47 have succeeded in both identification and grasping tasks, where 2 failures are due to identification and 1 failure is due to grasping. The overall success rate is 94%, which proves the feasibility of the gripper in searching and grasping through tactile perception.

Field Test

An important application of JamTac is grasping in low-visibility environments, especially in turbid water. To test its performance in real environments, a piece of handheld underwater salvage equipment is developed as shown in Figure 10A. In this equipment, JamTac is connected to a telescopic carbon fiber stick through a Cardan joint. The diameter of the gripper membrane is 10 cm, and the length of the stick is 55–160 cm. The purpose of the Cardan joint is to allow the gripper to stay upright when salvaging in a farther area (Fig. 10B). The pumping devices and batteries are contained in a backpack. Besides, a cell phone is mounted on the operator's wrist, which can show the real-time image from the RGB camera inside the gripper through Wi-Fi. And an radio-frequency wireless push button switch in the operator's hand can control the grasping and releasing operation of the gripper. The entire equipment is portable, which can be carried and operated by a single person conveniently.

With this equipment, two underwater salvage experiments were carried out (Supplementary Movies S6, S7, and Fig. 10C). One was performed in a pool, and the other in a sewer well. A screwdriver was used for the test. The screwdriver was thrown into the water, and then the operator started searching with the equipment around the falling area. As shown in Figure 10C, the object can be seen clearly when it is detected. Once making sure that the object is in firm contact with the gripper, the operator pressed the button to grasp the object. It should be noted that the water is turbid in both cases where the sunk object cannot be observed through the water at all. Both experiments succeeded, which validate the feasibility of JamTac in real applications. As far as we know, this might be the first tactile gripper that has been successfully applied in turbid water salvage.

Conclusion

A tactile jamming gripper with high-resolution tactile sensing capability is proposed, which uses the principle of jamming particles and vision-based tactile detection technology. To improve the perception accuracy of the gripper, we innovatively design the gripper from many aspects, including the method of acquiring tactile information, the

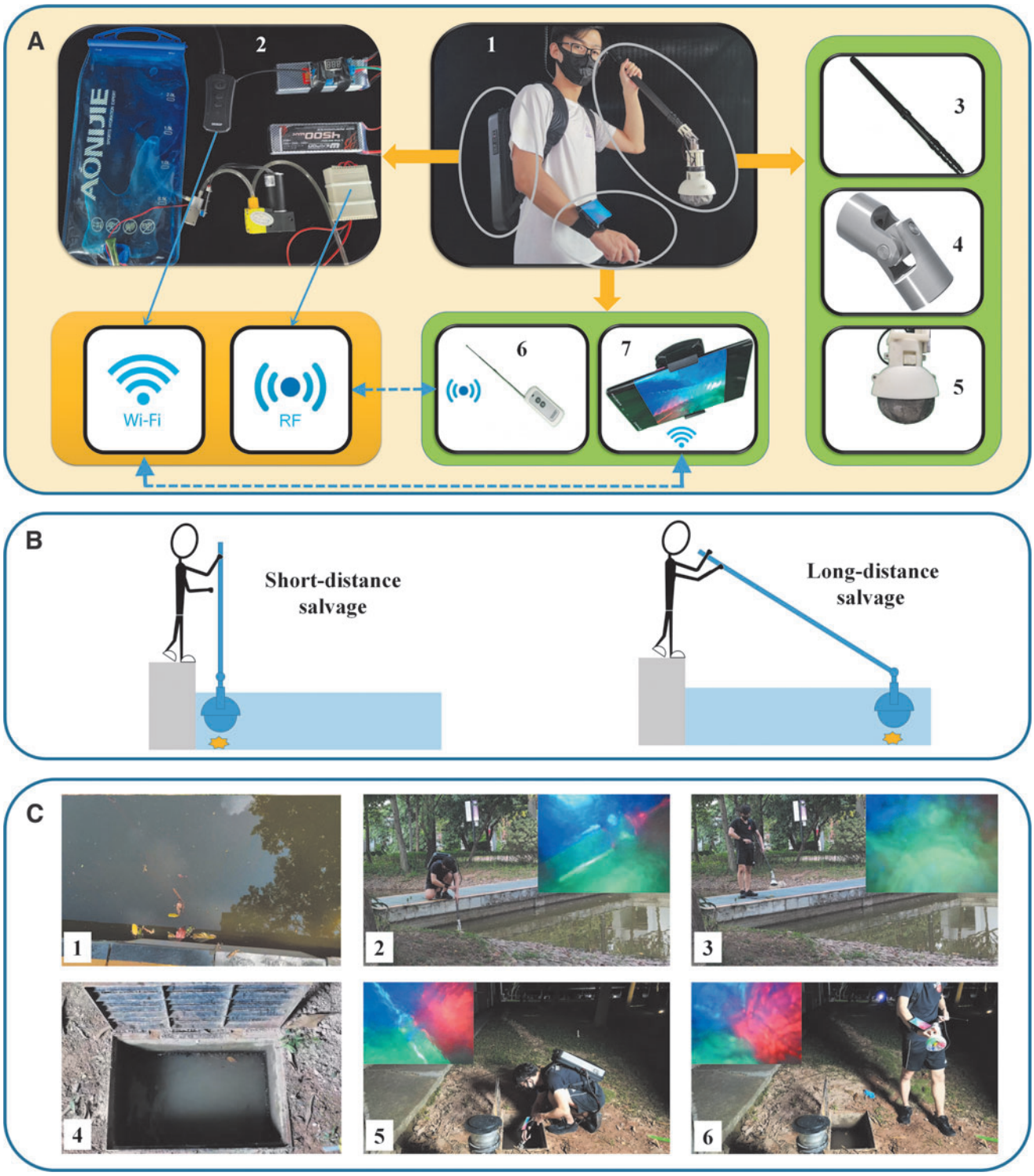

FIG. 10. Underwater salvage equipment and experiments. **(A)** Field test equipment. 1: The handheld underwater salvage equipment carried by a person. 2: The backpack contains batteries, liquid pumping devices, an RF module, and a Wi-Fi module. 3: Telescopic carbon fiber stick. 4: Cardan joint. 5: JamTac. 6: Two-button 433 MHZ wireless RF switch. 7: Cell phone in the holder. **(B)** Usage of the equipment. **(C)** Underwater salvage experiments. 1: A close view of the pool. 2: Underwater salvage in the pool. 3: Pool salvage done. 4: A close view of the sewer well. 5: Underwater salvage in the sewer well. 6: Sewer salvage done.

internal padding of the gripper, the material of the elastic membrane, and the internal optics. Compared with other existing grippers, the presented gripper not only has excellent grasping ability but also has multiple-source perception capability of force, shape, texture, and hardness.

Experimental results show that the force perception accuracy of JamTac is about 0.155 N (RMSE), the shape/texture recognition accuracy achieves 98.8%, and the hardness detection accuracy achieves 100%. The gripper also reaches an overall success rate of 94% in the autonomous searching and grasping experiment. The results indicate that JamTac has achieved high-quality tactile perception.

The underwater salvage experiments in real environments show a promising application field for JamTac. However, we also found some problems that need to be improved in the future. First, the grasping speed is slow now. Using a high-speed pump may solve this problem. Second, JamTac is more suitable for grasping objects on a flat and hard surface. Improving its efficiency in more complicated environments such as silt is of great value. Third, JamTac cannot grasp objects suspended in water. This may be solved using a pair of grippers to work as a jaw.

Acknowledgments

The authors thank Jiatai Guo for experiment assistance, Jiawei Zhang and Linrui Zhang for the help of image processing implementation, and Jiayi Li for diagram drawing assistance.

Data and Materials Availability

The data that support this research are available at https://drive.google.com/drive/folders/1G4ah1PxAd9Dmly69RnW6MvAi_mUfGZUn?usp=sharing , which comprise raw images for the experiments.

Author Disclosure Statement

No competing financial interests exist.

Funding Information

This work was supported by the National Natural Science Foundation of China (Nos. 62003188 and U1813216), Guangdong Special Branch Plan for Young Talent with Scientific and Technological Innovation (No. 2019TQ05Z111), China Postdoctoral Foundation (No. 2020M670335).

Supplementary Material

Supplementary Data
Supplementary Figure S1
Supplementary Table S1
Supplementary Movie S1
Supplementary Movie S2
Supplementary Movie S3
Supplementary Movie S4
Supplementary Movie S5
Supplementary Movie S6
Supplementary Movie S7

References

1. Johansson RS, Flanagan JR. Coding and use of tactile signals from the fingertips in object manipulation tasks. Nat Rev Neurosci 2009;10:345–359.
2. Lee J, Hwangbo J, Wellhausen L, *et al.* Learning quadrupedal locomotion over challenging terrain. Sci Robot 2020; 5:eabc5986.
3. Calandra R, Owens A, Upadhyaya M, *et al.* Levine, The feeling of success: Does touch sensing help predict grasp outcomes? ArXiv Preprint, ArXiv:1710.05512 2017.
4. Lin Y, Sun Y. Robot grasp planning based on demonstrated grasp strategies. Int J Robot Res 2015;34:26–42.
5. Wang Z, Li Z, Wang B, *et al.* Robot grasp detection using multimodal deep convolutional neural networks. Adv Mech Eng 2016;8:1687814016668077.
6. Karaoguz H, Jensfelt P. Object detection approach for robot grasp detection. In: IEEE International Conference on Robotics and Automation. Montreal, QC, Canada: IEEE, 2019, pp. 4953–4959.
7. Xu W, Zhang H, Yuan H, *et al.* A compliant adaptive gripper and its intrinsic force sensing method. IEEE Trans Robot 2021;37:1584–1603.
8. Maria GD, Natale C, Pirozzi S, Force/tactile sensor for robotic applications. Sens Actuat A Phys 2012;175:60–72.
9. Zou L, Ge C, Wang ZJ, et al Novel tactile sensor technology and smart tactile sensing systems: A review. Sensors 2017;17:2653.
10. Wu Y, Liu Y, Zhou Y, *et al.* A skin-inspired tactile sensor for smart prosthetics. Sci Robot 2018;3:eaat0429.
11. Ma Y, Liu N, Li L, *et al.* A highly flexible and sensitive piezoresistive sensor based on MXene with greatly changed interlayer distances. Nat Commun 2017;8:1–8.
12. Li T, Luo H, Qin L, *et al.* Flexible capacitive tactile sensor based on micropatterned dielectric layer. Small 2016;12:5042–5048.
13. Du L, Zhu X, Zhe J. An inductive sensor for real-time measurement of plantar normal and shear forces distribution. IEEE Trans Biomed Eng 2014;62:1316–1323.
14. Lepora NF. Soft biomimetic optical tactile sensing with the TacTip: A review. IEEE Sens J 2021;21:21131–21143.
15. Kamiyama K, Kajimoto H, Kawakami N, *et al.* Evaluation of a vision-based tactile sensor. In: IEEE International Conference on Robotics and Automation. New Orleans, LA, USA: IEEE, 2004, pp. 1542–1547.
16. Lambeta M, Chou PW, Tian S, *et al.* DIGIT: A novel design for a low-cost compact high-resolution tactile sensor with application to in-hand manipulation. IEEE Robot Autom Lett 2020;5:3838–3845.
17. Yuan W, Dong S, Adelson EH. Gelsight: High-resolution robot tactile sensors for estimating geometry and force. Sensors 2017;17:2762.
18. Padmanabha A, Ebert F, Tian S, *et al.* Omnitact: A multi-directional high-resolution touch sensor. In: IEEE International Conference on Robotics and Automation. Paris, France: IEEE, 2020, pp. 618–624.
19. Ward-Cherrier B, Pestell N, Cramphorn L, *et al.* The Tactip family: Soft optical tactile sensors with 3d-printed biomimetic morphologies. Soft Robot 2018;5:216–227.
20. Sun H, Kuchenbecker KJ, Martius G. A soft thumb-sized vision-based sensor with accurate all-round force perception. Nat Mach Intell 2022;4:135–145.
21. Ward-Cherrier B, Rojas N, Lepora NF. Model-free precise in-hand manipulation with a 3d-printed tactile gripper. IEEE Robot Autom Lett 2017;2:2056–2063.
22. Ward-Cherrier B, Cramphorn L, Lepora NF. Tactile manipulation with a TacThumb integrated on the open-hand M2 gripper. IEEE Robot Autom Lett 2016;1:169–175.
23. Pang C, Mak K, Zhang Y, *et al.* Viko: An adaptive Gecko gripper with vision-based tactile sensor. In: IEEE International

Conference on Robotics and Automation. Xi'an, China: IEEE, 2021, pp. 736–742.
24. Van Duong L. Large-scale vision-based tactile sensing for robot links: Design, modeling, and evaluation. IEEE Trans Robot 2020;37:390–403.
25. Kuppuswamy N, Alspach A, Uttamchandani A, *et al.* Soft-bubble grippers for robust and perceptive manipulation. In: IEEE/RSJ International Conference on Intelligent Robots and Systems. Las Vegas, NV, USA: IEEE, 2020, pp. 9917–9924.
26. Kim YJ, Song H, Maeng CY. Blt gripper: An adaptive gripper with active transition capability between precise pinch and compliant grasp. IEEE Robot Autom Lett 2020; 5:5518–5525.
27. Yuan S, Shao L, Yako CL, *et al.* Salisbury, design and control of roller grasper V2 for in-hand manipulation. In: IEEE/RSJ International Conference on Intelligent Robots and Systems. Las Vegas, NV, USA: IEEE, 2020, pp. 9151–9158.
28. Shaqura M, Shamma JS. A novel gripper design for multi hand tools grasping under tight clearance constraints and external torque effect. In: IEEE International Conference on Mechatronics and Automation. Takamatsu, Japan: IEEE, 2017, pp. 840–845.
29. Andrychowicz M, Baker B, Chociej M, *et al.* Learning dexterous in-hand manipulation. Int J Robot Res 2020;39: 3–20.
30. Chen W, Xiong C, Wang Y. Analysis and synthesis of underactuated compliant mechanisms based on transmission properties of motion and force. IEEE Trans Robot 2020;36:773–788.
31. Galloway KC, Becker KP, Phillips B, *et al.* Soft robotic grippers for biological sampling on deep reefs. Soft Robot 2016;3:23–33.
32. Li H, Yao J, Zhou P, *et al.* High-load soft grippers based on bionic winding effect. Soft Robot 2019;6:276–288.
33. Miron G, Bédard B, Plante JS. Sleeved bending actuators for soft grippers: A durable solution for high force-to-weight applications. Actuators 2018;7:40.
34. Manti M, Hassan T, Passetti G, *et al.* A bioinspired soft robotic gripper for adaptable and effective grasping. Soft Robot 2015;2:107–116.
35. Al Abeach LAT, Nefti-Meziani S, Davis S. Design of a variable stiffness soft dexterous gripper. Soft Robot 2017;4: 274–284.
36. Liu SQ, Adelson EH. GelSight Fin Ray: Incorporating tactile sensing into a soft compliant robotic gripper. In: IEEE International Conference on Soft Robotics. Edinburgh, United Kingdom: IEEE, 2022, pp. 925–931.
37. Zhao H, O'Brien K, Li S, *et al.* Optoelectronically innervated soft prosthetic hand via stretchable optical waveguides. Sci Robot 2016;1:eaai7529.
38. Truby RL, Della Santina C, Rus D. Distributed proprioception of 3D configuration in soft, sensorized robots via deep learning. IEEE Robot Autom Lett 2020;5:3299–3306.
39. Gu G, Zhang N, Xu H, *et al.* A soft neuroprosthetic hand providing simultaneous myoelectric control and tactile feedback. Nat Biomed Eng 2023;7:589–598.
40. Cui Y, Liu XJ, Dong X, *et al.* Enhancing the universality of a pneumatic gripper via continuously adjustable initial grasp postures. IEEE Trans Robot 2021;37:1604–1618.
41. Hussain I, Malvezzi M, Gan D, *et al.* Compliant gripper design, prototyping, and modeling using screw theory formulation. Int J Robot Res 2021;40:55–71.
42. Linghu C, Zhang S, Wang C, *et al.* Universal SMP gripper with massive and selective capabilities for multiscaled, arbitrarily shaped objects. Sci Adv 2020;6:eaay5120.
43. Brown E, Rodenberg N, Amend J, *et al.* Universal robotic gripper based on the jamming of granular material. Proc Natl Acad Sci U S A 2010;107:18809–18814.
44. Amend JR, Brown E, Rodenberg N, *et al.* A positive pressure universal gripper based on the jamming of granular material. IEEE Trans Robot 2012;28:341–350.
45. Fitzgerald SG, Delaney GW, Howard D. A review of jamming actuation in soft robotics. Actuators 2020;9:104.
46. Howard D, O'Connor J, Brett J, *et al.* Shape, size, and fabrication effects in 3D printed granular jamming grippers. In: IEEE International Conference on Soft Robotics. New Haven, CT, USA: IEEE, 2021, pp. 458–464.
47. Amend J, Cheng N, Fakhouri S, *et al.* Soft robotics commercialization: Jamming grippers from research to product. Soft Robot 2016;3:213–222.
48. Licht S, Collins E, Mendes ML, *et al.* Stronger at depth: Jamming grippers as deep sea sampling tools. Soft Robot 2017;4:305–316.
49. Platkiewicz J, Lipson H, Hayward V. Haptic edge detection through shear. Sci Rep 2016;6:1–10.
50. Hughes J, Iida F. Tactile sensing applied to the universal gripper using conductive thermoplastic elastomer. Soft Robot 2018;5:512–526.
51. Sakuma T, Drigalski FV, Ding M, *et al.* A universal gripper using optical sensing to acquire tactile information and membrane deformation. In: IEEE/RSJ International Conference on Intelligent Robots and Systems. Takamatsu, Japan: IEEE, 2018, pp. 1–9.
52. Budwig R. Refractive index matching methods for liquid flow investigations. Exp Fluids 1994;17:350–355.
53. Kragh H. The Lorenz-Lorentz formula: Origin and early history. Substantia 2018;2:7–18.
54. Chen Y, Lin J, Du X, *et al.* Non-destructive fruit firmness evaluation using vision-based tactile information. In: IEEE International Conference on Robotics and Automation. Philadelphia, PA, USA: IEEE, 2022.

Address correspondence to:
Xueqian Wang
Center of Intelligent Control and Telescience
Tsinghua Shenzhen International Graduate School
Tsinghua University
Shenzhen 518055
China

E-mail: wang.xq@sz.tsinghua.edu.cn

Bin Liang
Navigation and Control Research Center
Department of Automation
Tsinghua University
Beijing 100084
China

E-mail: bliang@tsinghua.edu.cn